

Towards a Knowledge guided Multimodal Foundation Model for Spatio-Temporal Remote Sensing Applications

Praveen Ravirathinam*

University of Minnesota, Twin Cities
Minneapolis, United States
pravirat@umn.edu

Rahul Ghosh*

University of Minnesota, Twin Cities
Minneapolis, United States
ghosh128@umn.edu

Ankush Khandelwal*

University of Minnesota, Twin Cities
Minneapolis, United States
khand035@umn.edu

Vipin Kumar

University of Minnesota, Twin Cities
Minneapolis, United States
kumar001@umn.edu

Abstract

In recent years, there is increased interest in foundation models for geoscience due to vast amount of earth observing satellite imagery. Existing remote sensing foundation models make use of the various sources of spectral imagery to create large models pretrained on masked reconstruction task. The embeddings from these foundation models are then used for various downstream remote sensing applications. In this paper we propose a foundational modeling framework for remote sensing geoscience applications, that goes beyond these traditional single modality masked autoencoder family of foundation models. This framework leverages the knowledge guided principles that the spectral imagery captures the impact of the physical drivers on the environmental system, and that the relationship between them is governed by the characteristics of the system. Specifically, our method, called MultiModal Variable Step Forecasting (MM-VSF), uses multimodal data (spectral imagery and weather) as its input and a variable step forecasting task as its pre-training objective. In our evaluation we show forecasting of satellite imagery using weather can be used as an effective pretraining task for foundation models. We further show the effectiveness of the embeddings from MM-VSF on the downstream task of pixel wise crop mapping, when compared with a model trained in the traditional setting of single modality input and masked reconstruction based pretraining.

Keywords

Foundation model, Spatiotemporal modelling, Remote Sensing, Knowledge guided

1 Introduction

Increased availability and ease of access to large scale satellite data has motivated the development of deep learning models that use this data to perform tasks such as land cover mapping[8, 14, 23], wildfire mapping [20, 24, 32], crop yield prediction [15, 30], flood forecasting[3] etc. In more recent times, methods have been developed to use large amounts of data in a self supervised fashion to pretrain their model weights using a pretraining task, such as masked reconstruction [10], which would then be finetuned for downstream tasks. Such models, called foundation models, have been shown to generalise their embeddings over various tasks,

*These authors contributed equally to this research.

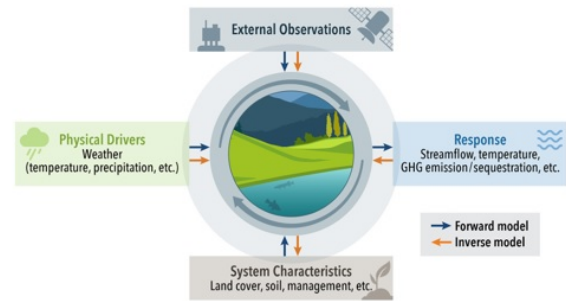


Figure 1: Abstract Representation of an Environmental System

called downstream tasks, in the image [25, 31] and text domains[27] (e.g. large language model such as GPT [1]). Motivated by the success of such models, there is a huge interest in building foundation models for geoscience applications[2, 4, 6, 9, 11–13, 17, 18]. Most geoscience foundation models can be placed into one of two groups based on the data they use : (1) weather-climate [21, 22] that are typically used for weather forecasting or climate modeling and (2) spectral data from remote sensing satellites [5, 12] that are largely used for identifying land-use land-cover change dynamics. The focus of this paper is on the land-use land cover applications that are typically handled by remote sensing foundation models. Such remote sensing foundation models are typically built using the vast amounts of spectral data from various satellites available using a pretraining task such as masked reconstruction [4, 5, 7, 16, 19, 26]. However, these methods do not account for interrelationships that exist between different components of the environmental systems.

If one is to envision the environment as a system, it can be thought of as various physical drivers such as weather, moisture, etc. act upon a region (e.g. a farm, catchment) that has physical properties such as land cover type, soil characteristics, etc. to result in a response such as crop growth, streamflow, emissions which can be observed by sensors and satellites such as Sentinel, Landsat etc. This broad picture is captured in Figure 1 and is called the forward process. However, if one is interested in properties such as land cover type, the inverse process can be used to infer these values given the physical drivers, sensor observations, and possibly the

system response[23]. To the best of our knowledge, most existing remote sensing foundation models currently use only the spectral imagery in their pretraining as well as downstream tasks [5, 12], thus leaving out the key information that the spectral imagery captures the impact of the physical drivers on the environmental system, and the relationship between them (and other observables such as crop yield or stream flow) is governed by the characteristics of the system (e.g., land cover type, crop management). In this work, we show how to realise this vision in both the pretraining and downstream task. Our proposed approach differs from existing work along several dimensions as outlined below.

Remote sensing based foundation models are usually built using one modality of data, which is typically spectral imagery [4, 26, 29]. However, from Figure 1, we can see that various components interact with each other leading to interesting phenomena. For example, weather acts on a crop field which leads to crop growth, which is seen by satellite imagery. Such examples highlight the need to capture interactions between physical components and drivers in the foundation model, which are not included in the pretraining tasks of existing geoscience models. In our approach, we include both spectral imagery and weather in our pretraining task to ensure that the interaction between these components is captured in the embeddings of our model. In particular, we show how to include weather in the pretraining task of forecasting and how its inclusion benefits the downstream task of pixel wise crop mapping.

Majority of remote sensing based foundation model methods use masked reconstruction as their pretraining task [12, 28]. However, by leveraging the scientific knowledge about the interrelationships between different components of the environmental system, we can go beyond this pretraining task. In particular, using the forward process, we can see forecasting of satellite imagery as a potential pretraining task. Without the use of weather, forecasting of satellite imagery would not be very effective, but with its inclusion it may be possible the model would be able to use this weather data to effectively forecast an image, and in the process create much more meaningful embeddings as compared to reconstruction. In this work, we present a methodology for the pretraining task of satellite image forecasting with weather and show how it improves the embeddings and in turn the performance on downstream tasks.

Another major feature of remote sensing satellite data is its spatio temporal nature. Most of the remote-sensing downstream tasks (crop classification, land-use land cover change detection, crop yield prediction) require such a spatiotemporal input, however their required time-scales may vary. For example crop mapping requires a much longer time scale than land-use land cover (LULC) change detection. Most foundation models built for geoscience, either do not account for the temporal nature of satellite data or are limited to processing the temporal data of a fixed length [12]. For a unified foundation model it is important to not only include mechanisms that take advantage of the temporal nature of remote sensing data in their approach, but also have temporal flexibility in the length of its input, especially for generalizing across various downstream tasks.

In this paper, we present a novel spatio temporal multimodal foundation model that uses knowledge guided concepts to strengthen its embeddings. We call our approach MultiModal Variable step

Forecasting (MM-VSF), that uses both satellite and weather data (two entirely different modalities) to perform the pretraining task of forecasting (variable forecasting) and show how the embeddings created by our approach are richer when compared to those created using the task of reconstruction. We also present a temporally flexible architecture that efficiently makes use of the temporal nature of both satellite and weather data to give results that go beyond simple temporal autocorrelation of satellite data. We show how the embeddings created by our pretraining method generalise better for the downstream task of crop mapping when compared to other pretraining methods.

2 Method

Like most existing foundational models for geoscience, our architecture also follows a heavy encoder and lightweight decoder format. Keeping our decoder lightweight forces the embedding created by the encoder to be rich enough to solve the pretraining task and in turn would be rich for various downstream tasks. Unlike previous methodologies we incorporate multiple modalities into our pretraining, namely spectral imagery and weather.

2.1 Pretraining Task

The most common pretraining task in geoscience has been reconstruction of spectral imagery. To enrich the embedding created, typically varying amounts of the input spectral image are masked, making the reconstruction task of the entire image harder leading to better embeddings. However, simple reconstruction embeddings capture just that particular image and might not be suited for downstream tasks that rely on multi temporal contexts such as crop mapping or land cover land use change. To solve this, previous works included multiple timestamps in their input, however most of these methods stacked these images together [12], thus removing the temporal aspect. However, some methods added a timestamp positional embedding so that the model has a sense of time [13]. This led to moderate success in handling downstream tasks that require multi temporal contexts.

Another common pretraining task is forecasting of imagery. Typically, this pretraining task has been used in weather related foundation models and not in spectral imagery based foundation models. Foundation models created using masked forecasting has shown great success in weather related downstream tasks [21, 22]. To enrich the embeddings created, these works add variable future time forecasting, i.e vary the amount of time into the future the model needs to forecast to. This pretraining task using just spectral imagery would not make much sense, as it would be very challenging to predict how an image would look in the future based on just one image and a future time. At the minimum we would need more information such as geographic location, time of year, country etc.

In our work, we combine these pretraining tasks in a unique multimodal fashion. From Figure 1, we have seen that various components of the environment interact with each other. Additionally, it has been shown in the past that inclusion of weather has led to improved results in downstream geoscience tasks [23]. Thus we propose to include weather in the pretraining task. One simple strategy is to add weather as an additional modality to reconstruct in the pretraining task. However, this method does not infuse weather

dynamics into the embeddings. That is why we propose using multimodal forecasting as a pretraining task. Our idea is to use the current satellite imagery and provide weather data till a particular day on which we would ask the model to predict the satellite image at that point in the future. Asking the model to predict a satellite image in the future without any weather information would be sub-optimal, but providing weather can help the model narrow down the search space in figuring out how the land cover would change. For example, if there was a lot of rain, the lakes would be fuller, if there was a lot of sunlight then growth of crop/other vegetation would accelerate. As a result, pretraining in this future image prediction scheme would infuse land growth/change dynamics into the embeddings that the model creates. Our hypothesis is that this extra knowledge infusion would help greatly in downstream tasks that rely on land growth and change dynamics such as crop prediction, land cover land use change, etc.

To summarise, our proposed pretraining task is to predict a spectral image in the future (response) using a series of spectral images in the past (context) along with the weather till the future date (query) we want to predict. We call this pretraining task as Variable step Forecasting (*VSF*), where the model is expected to forecast k steps into the future. During pre-training, k is chosen randomly for different instances. During inference, k is specified by the user. We also mask out patches in the spectral imagery to make the prediction harder and lead to better embeddings. We will describe our masking strategy for pretraining in a future section.

2.2 Dataset

Our dataset consists of Sentinel imagery for spectral imagery and ERA5 land analysis data for our weather component. We chose these two sources due to their temporal resolutions and more importantly their availability globally. Due to these factors, we randomly sampled around 10000 locations across land areas globally. Each location is of size 128x128 Sentinel pixels and for spectral imagery we collected all images for that region in that year. Due to missing data and improper coverage of some regions, the number of Sentinel samples from each region would vary. For example, regions in well covered regions such as US, might have upto 70 image instances in a year for that region, whereas regions like India might not be as well covered and would have 40 image instances. For each instance, we collect six bands namely (B2, B3, B4, B8, B9, B12), bands which have shown to be the most useful in land cover related tasks as well as have been used in other works. For each image instance, we also collect the day of the year it came from, thus forming a series with a length the same as the number of image instances for that location with each element having a value between 1 and 365. We get our weather data from ERA5 Land Daily Aggregates. This globally available data source consists of various bands that are useful for land cover related tasks. To keep it simple and data efficient we chose 5 bands from this dataset, namely (temperature 2m min, temperature 2m max, total precipitation sum, u component of wind 10m, v component of wind 10m). The frequency of this data is daily and it is available at a resolution of 11k meters, a very coarse resolution compared to the Sentinel pixels. Given the coarse resolution, for most patches in our analysis we get only one value

band set per timestamp, thus making our weather data of length 365 with 5 values per timestamp.

To summarise, for each location our data comprises of 3 main components:

- Spectral Imagery Series: A series of Sentinel2 Imagery each of 6 bands and of shape 128x128. Length of this series depends on coverage of the location.
- Weather Data Series: A series of ERA5 Land data of 5 bands and of shape 1x1, with a series length of 365 (one per day)
- Day of Year Series: A series of the day of the year number for each spectral image in the series. The length of this series is same as the spectral imagery series.

2.3 Architecture

Figure 2 depicts *MM-VSF*'s architecture diagram. Since our task is forecasting, we need an architecture that is able to capture various modalities of the data at hand. This includes spatial and temporal modalities of satellite data, temporal modality of weather data as well how these modalities interact with each other.

For extracting the spatial features from the spectral imagery we use a vision transformer (ViT). ViT have been shown to be very useful in extracting important spatial features [10], even in the geoscience context [12] and in the presence of high masking. ViT encoder takes a single spectral image and converts into a patch grid of embedding size of your choice. Now given that our input is an image series, we propose using a shared ViT to extract spatial embedding from spectral imagery of each input timestamp. This would lead to a robust encoder, as it has to learn how to embed images from all timestamps in a fashion that is suitable for forecasting. For each timestamp image, we get embeddings on the unmasked patches of our defined dimension. We also make use of patch positional embedding in this stage. In summary, from this stage we are left with a series of spectral image embeddings on unmasked patches for each timestamp.

As mentioned before, due to the coarse resolution of the weather data, for each image location, we only have one weather data value per time-stamp. Therefore, we need only a temporal embedding method and dont need any spatial component. For encoding our weather data we use a bidirectional LSTM. We initially tried using a temporal transformer instead of an LSTM, but this led to poor reconstruction and in turn poor embeddings. Even when trying to solely reconstruct masked weather, LSTM based approaches proved to have higher accuracy in reconstruction over the transformer based approaches. We use the LSTM based approach to get a weather embedding for each timestamp, and then subsample from this series the weather embeddings corresponding to the input image timestamps, in a fashion similar to WSTAT[23]. We call this extraction and matching of embeddings temporal embedding matching.

From the input to the model, we have a series of the day of the year values for the spectral images in the input as well as the final forecast image day of year. It has been shown in other work that inclusion of the day of year information in the embedding has led to improvement of results by giving the embedding a context of the absolute time. So to incorporate this in our architecture, we use a shared linear layer with tanh activation that takes the day of the year and gives an embedding of our specified dimension. So we will

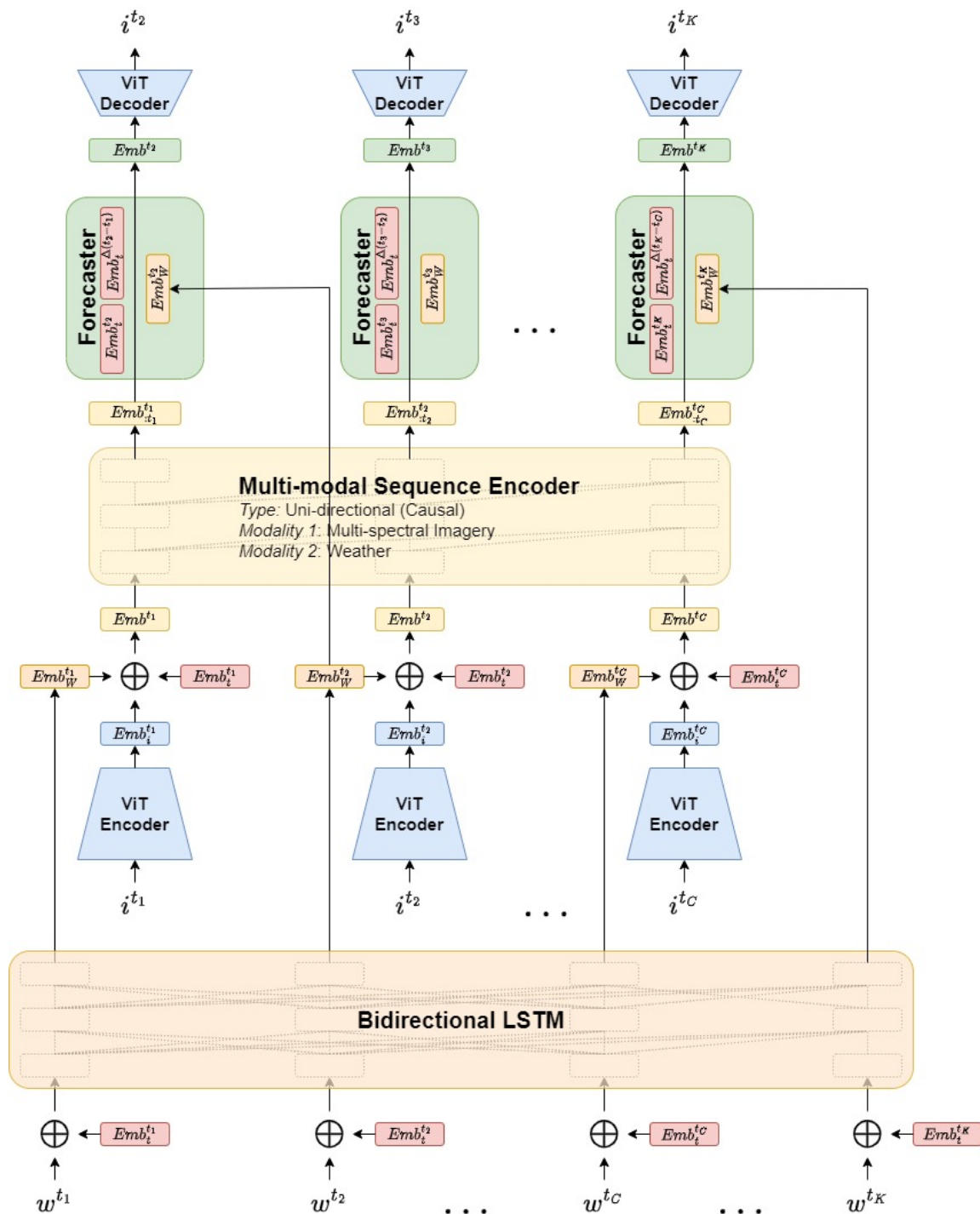


Figure 2: MultiModal Variable step Forecasting (MM-VSF) Architecture diagram

have a series of embeddings of our specified dimension where each embedding corresponds to the day of the year. We will use these

embeddings later on to provide certain components with information about day of year. Orthogonally, using the raw day of year

values, we can create another series that corresponds the number of days in between the images, i.e the delta in timestamps. Similar to how we created an embedding for day of year values, we can also create a series for the delta timestamps series. Such embeddings for delta days have been shown to be useful in forecasting tasks [21]. As a result, here as well we apply a linear layer followed by tanh on the delta timestamp values to create a delta timestamps embedding series. This embedding series will be used in the forecasting components of our architecture to provide information about how far to forecast.

From the previous steps, we now have a two time series of embeddings, one with each element of the series corresponding to the spatial embeddings of a particular timestamp and the other series corresponding to the temporally matched weather embeddings. We also have the series of embeddings for the day of year timestamps. Since all these series are of the same length, we add them all along the temporal dimension to create a multimodal embedding series. This multimodal embedding series, is still however, temporally unbound, i.e there is no temporal relation between the embeddings. So to extract the temporal embeddings, we use a BERT style transformer, with forward only attention. We run the temporal series analysis on embedding patches that come from the same spatial location in the overall image. Due to our uniform spatiotemporal masking, the number of such embedding patches across all locations should be the same, which is dependant on the amount of masking one does. For example, if there are 6 images in the series and the masking is 50%, then in the temporal transformer would have 3 inputs in its series. Now across spatial patches, the timestamps from which these embeddings come will vary. This feature allows our temporal transformer to learn robust embeddings using the multimodal information from the combination of the spectral image embedding information, weather embedding information and the day of the year embedding information. Another important aspect here is that we make sure that there only forward attention present in the temporal transformer, i.e the temporal embeddings created are not bidirectional in nature. This feature makes sure there is no information leakage from future timestamp information to previous timestamps embeddings. Therefore following this stage, we are left with a series of embeddings $Emb_{STW} = [Emb_{:t_1}^t, \dots, Emb_{:t_C}^t]$. Any downstream task will use this embedding series for finetuning. Depending on the task, one can choose to all use embeddings or choose to use only the final embedding. Another thing to remember is that while finetuning, typically no masking is present, so there will be more features per timestamp embedding.

Now our pretraining task is forecasting, so let us now delve into the decoder part of the foundation model. The most obvious way to do forecasting is to take the final embedding of the series Emb_{STW} and use it to forecast an image in the future. However, we can go a step further, as since our embeddings are constructed in a forward only method, we can use each of the embeddings to forecast an image in its respective future (i.e in a day of the year past the day of the year of the corresponding embedding from the input series). So apart from choosing a day of the year in the future for the final timestamp to forecast, we can also choose intermediate days for the rest of the embeddings in the series to forecast. There are many ways to choose these intermediate days, but the most

straightforward and computationally least expensive are the day of year days of the input series but one timestamp shifted, i.e the embedding that corresponds to timestamp t_1 of the input series would be used to forecast the image at day of year timestamp t_2 from the input series, embedding of timestamp t_2 would be used to forecast image at timestamp t_3 and so on. Such multiple forecasting allows for the decoder to be more robust, as similar to encoder, the decoder also has shared weights across timestamps. So we can get a series of future day of year numbers for our forecast and also calculate the delta days series as well. We can use the same tanh and Linear layers as before to get the forecast day of year embedding series and the forecast delta days embedding series. We can also use the forecast day of year numbers to get the weather embeddings for those corresponding days, similar to the temporal embedding matching process in the encoder. The logic here is that, with the current image embedding and weather information till the day of the year to forecast to, the model can predict how the image would look in the future. Expecting a future image to look accurate with no information apart from day of year would be very feasible, but with weather information until that day, it is possible to estimate how it might look. For example, if there was a lot of rain in that period, then water bodies might have grown, or if there was a lot of sunlight, crop growth would have accelerated etc. All this is made possible by the inclusion of weather, which ties back to our original hypothesis that inclusion of weather would lead to stronger embeddings.

Following these steps we have four embedding series, which we add together, to form the basis embedding series on which forecasting is to be done. Now on these embeddings, we apply a series of linear layers and activations to act as the forecaster. The point of these layers is to morph the embedding from the initial timestamp space to the future timestamp space using the information from the image embedding and weather data before passing the embedding to the decoder. We found that including these layers led to great benefits in terms of performance on pretraining task, as these layers help in giving more depth to the embeddings.

Following this stage, we repopulate these embeddings in their respective unmasked positions in the timestamps and zero out the masked patches to pass to the decoder, as done by most methods in transformer based autoencoder methods[10, 12]. We use a lightweight decoder (similar to the one used in ViT) to ensure that the main focus of the model is to create good embeddings with the encoder to capture the best information so that even a lightweight decoder can perform the pretraining task required. Also, in any downstream task, we would need the embeddings from the encoder and the decoder would not be used. Similar, to the encoder, we have only one shared vision transformer in the decoder that performs the operations on each timestamp using the same weights. Following the vision transformer, we have a linear layer to bring the values back to the spectral image space and reshape the output to match the required size of the spatiotemporal stack.

2.4 Masking

Since we are dealing with a spatiotemporal based input, we adopt to using a spatiotemporally uniform masking method. Previous methods mainly adopt to random masking of patches and do not

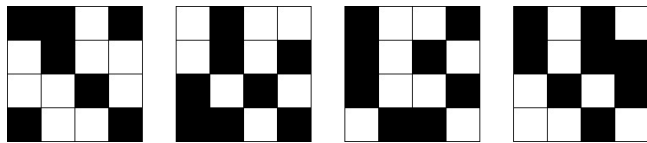


Figure 3: Example of 50 percent spatiotemporally uniform masking on a 4x4 image timeseries of 4 timestamps

account for the temporal aspect. Since our proposed architecture has both spatial and temporal components, we needed a masking method that is fair both spatially and temporally. In our masking strategy, there are an equal number of masked patches per timestamp as well as an equal number of masked patches at each spatial patch location along the temporal axis. Figure 3 shows an example of such masking for a image series of 4 4x4 grids with 50% masking. From the Figure, we can see that in each timestamp image there are 8 patches masked and if one focuses on a particular patch location along the temporal dimension one can notice that 2 patches are available. This ensures that all temporal patch series that can be created from unmasked patches at each patch location would be of same length, which eases the implementation of our temporal component. Also since, each timestamp individually has the same number of unmasked patches, the shared vision transformer will also have same number of outputs per timestamp.

2.5 Implementation details

For the pretraining phase, we choose an input series length 6 image, and selected a random image after the final image as the final image to forecast. We also use 50% spatiotemporally masking and a patch size of 8 for the vision transformer. Model was trained till convergence on 4 A100 Nvidia GPUs using Adam Optimizer and Mean Squared Error loss.

3 Experimental Evaluation

In this section we evaluate various aspects of our proposed foundational model framework. First, we evaluate the performance on the forecasting-based pretraining task and highlight some examples to show that our method’s embeddings are capturing aspects beyond just encoding the image. We further evaluate the performance of our embeddings when finetuned to the crop mapping downstream task. We compare our results with embeddings created using the reconstruction pretraining task.

3.1 Baselines

Table 1 depicts the choices for input series to architectures and choices for pretraining tasks for models. Recall that our model’s ($MM - VSF$) pretraining task is k steps variable forecasting (VSF) in the future, i.e $P2$ from the table, and our input series is multimodal (MM), both satellite data and weather data, i.e $I2$ from the table. However, from the table we can see that there are three other variations, based on input and pretraining task choices, as shown below.

- $SM - MAE$: Single Modality Masked AutoEncoder ($SM - MAE$) with the Input series as satellite data and the pretraining task of Masked Reconstruction, i.e ($I1, P1$)

Table 1: Choices of input and pretraining task for the model.

Input Choices	
I1	Single Modality (Satellite data)
I2	Multimodal (Satellite + Weather data)
Pretraining task Choices	
P1	Masked Reconstruction (MAE)
P2	Variable Step Forecasting (VSF)

- $MM - MAE$: MultiModal Masked AutoEncoder ($MM - MAE$) with the Input series as satellite data and weather data and the pretraining task of Masked Reconstruction, i.e ($I2, P1$)
- $SM - VSF$: Single Modality Variable step Forecasting ($SM - VSF$) with the Input series as Satellite data and the pretraining task of Variable Step Forecasting, i.e ($I1, P2$)

Note that the above combinations can be implemented by only changing the inputs and the loss functions, without significant architecture changes. Thus these variations, which we call baselines, can also be considered as ablations of different components of our model. Also note that $SM - MAE$ is closest to the existing remote sensing based foundation models (e.g., [5, 12, 26]), as they also use only satellite data and pretrain using MAE.

3.2 Pretraining Task: Forecasting

Here we evaluate the relative utility of using both weather and spectral data (MM) vs spectral data (SM) only on the forecasting-based pretraining task. With the help of a few examples, we illustrate that the embedding produced by $MM - VSF$ are more powerful than those $SM - VSF$, as $MM - VSF$ is able to capture the dynamic relationship between weather and the changes in the physical environment on the land captured by spectral data. Figure 4 shows a comparison of the images from these models, i.e $SM - VSF$ and $MM - VSF$, on 3 independent examples. Each row correspond to a sample, with the first 6 images corresponding to the satellite component of the input series to the model, the weather component is not shown in the image but is passed along with the satellite component (as shown in Figure 2). Now, the output would also be a series of 6 images, with the last image corresponding to a future day as specified in the user input (this is shown above the image in the groundtruth column). Note that Figure 4 only shows the final forecast image for each method, as this is where one would expect the most impact from using weather. Both schemes are able to construct earlier images quite well, although $MM - VSF$ can improve over $SM - VSF$ in most cases. Row 1 depicts an example of a crop field, with the final forecast image being 120 days following the 6th image in the input series. We can see that from the groundtruth image, that harvest has occurred in the circular fields and growth has happened in the top left corner field. Comparing the forecasted images from $SM - VSF$ and $MM - VSF$, we can see that $MM - VSF$ is able to capture both the harvest and the growth of the crops. We can also see that $SM - VSF$ is not able to capture these changes. This shows that the inclusion of weather allows the embeddings created by $MM - VSF$ to capture the land cover dynamics that are driven by weather. Such dynamics cannot be captured by $SM - VSF$,

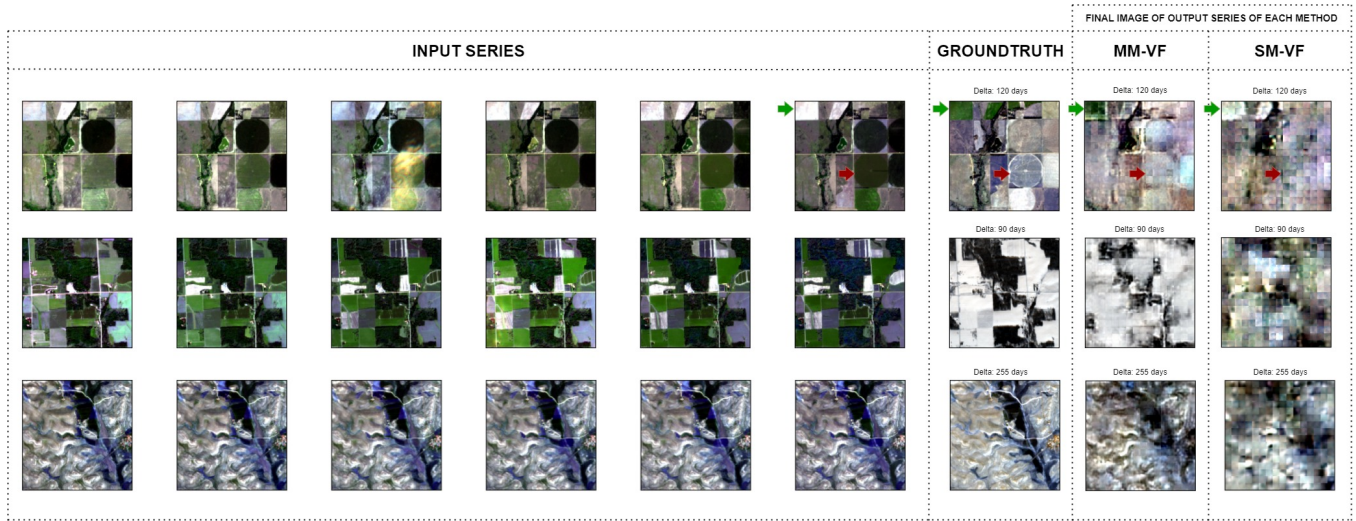


Figure 4: Forecast based Pretraining Task comparison. 50% Masking is not shown. Row 1 depicts a crop field with, Green arrows depict regions of growth, and Red arrows depict regions of harvest. Note how $MM - VSF$ captures both these phenomena better than $SM - VSF$. Row 2 depicts an example where $MM - VSF$ is able to add snowfall accurately compared to $SM - VSF$. Row 3 depicts an example where $MM - VSF$ does not include any land cover due to terrain but $SM - VSF$ adds false greenness

as it only has access to the past spectral imageries, and thus it can only capture temporal autocorrelation amongst the spectral images. Row 2 shows another example of a crop field later in the year, with the final forecast image being 90 days after the final image in the input series. We can see from the groundtruth image 90 days later that snow is present in the field, which is captured by $MM - VSF$ but not $SM - VSF$. This illustrates the ability of $MM - VSF$ to capture the relationship between precipitation and temperature (i.e., precipitation during cold winter days can fall as snow). $SM - VSF$ forecast shows a faded green field, which shows that it is not able to capture this relationship. One can also notice that evergreen regions within the forecasted image of $MM - VSF$ also have less snowfall when compared to the fields, showing that terrain information is also being captured. This is further reflected in Row 3, where a mountainous region is depicted and the final forecast image is 255 days following the final input image. We can see that even after 255 days there is not much change in the region, and this is correctly captured by our method ($MM - VSF$). $SM - VSF$ seems to add some greenness which is not present. These examples illustrate that inclusion of weather not only helps in predicting land cover change but also helps in identifying land cover terrain, and the model realises that some terrains no matter the weather do not change very much. Without weather, there is no way for the model to learn this which is reflected in the forecast image of $SM - VSF$. We further observe that all images from the forecast of $SM - VSF$ appear blocky, inspite of long periods of training. This can be explained as the model unable to forecast accurate images without weather information.

3.3 Downstream Task: Crop Mapping

Here we evaluate the performance of our proposed method ($MM - VSF$) in producing embeddings by fine-tuning to the crop mapping

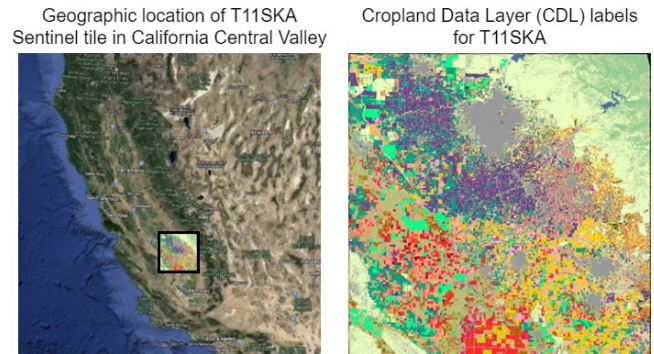


Figure 5: Geographic location of the T11SKA Sentinel Tile and its corresponding CDL labels. Each color in the CDL image corresponds to a land cover class.

downstream task. We compare our results with embeddings created using $SM - SAE$, which is the closest to the existing remote sensing foundation models.

3.3.1 Dataset and Region of Analysis. Our data for finetuning also comes from Sentinel2 and ERA5 land data. The region of analysis for testing our downstream task is the T11SKA tile in the California Central Valley, a region that is rich in crop cover and has been used for crop type mapping in various other works[]. Like other works, we get our land cover labels for this region from the Cropland Data Layer, an annually released land cover map for the entire continuous US by the USDA. A diagrammatic representation of the CDL labels and the geographic location of the T11SKA tile can be seen in Figure 5. As can be seen there are many crop classes present, making it a challenging region to map. Similar to WSTAT [23], we adopt a

Table 2: Comparison on downstream task of crop mapping across the pretraining tasks. Finetuning is done only using 2018 data

Crop class	2018		2019	
	$SM - MAE$	$MM - VSF$	$SM - MAE$	$MM - VSF$
Corn	0.7268	0.8409	0.4135	0.5708
Cotton	0.9663	0.9679	0.8346	0.9125
Winter_Wheat	0.7655	0.7928	0.1156	0.1777
Tomatoes	0.8719	0.888	0.768	0.7341
Grapes	0.8608	0.8638	0.7398	0.7543
Almonds	0.8073	0.789	0.3851	0.299
Walnut	0.8234	0.822	0.0238	0.5384
Pistachio	0.7667	0.7673	0.507	0.7003
Alfalfa	0.7207	0.7637	0.6892	0.7057
Grass	0.8564	0.8611	0.776	0.8445
Urban	0.5761	0.5552	0.6111	0.6191
Average	0.7947	0.8102	0.5331	0.6233

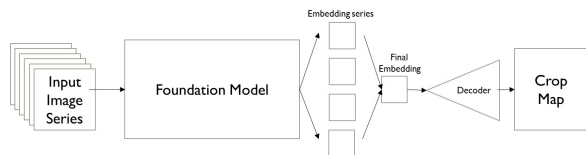


Figure 6: Layout of architecture for downstream task of crop mapping

grid based training method, by splitting the entire region into train, validation and test grids. We also follow their preprocessing steps including combination and erosion.

3.3.2 Crop mapping Architecture and Implementation details. Since crop mapping is a pixel wise output, we need an architecture that gives us a pixel wise output, in particular, we would need a decoder that takes the embedding series given by the foundation model encoder and constructs a pixel wise classification map using this series in a semantic segmentation fashion. Figure 6 shows a schematic of the downstream task architecture for crop mapping. The embedding series mentioned would correspond to the series Emb_{STW} , i.e the output series of the encoder. To map this embedding series to a pixel wise crop map, we follow an attention based approach, similar to WSTAT[23]. This strategy assigns a weightage to each timestamp embeddings and does an aggregated sum to form a multitemporal attention-based embedding. This multitemporal embedding is then acted by a series of upscaling and convolution layers with activation, then passed through an output Linear layer to form a pixel wise map.

For our input series, we chose to have 10 spectral images, bi-weekly from May to Sept, and while finetuning for crop mapping there is no masking of spectral imagery done. Note that the number of timestamps passed in the downstream task is different from the number passed during pretraining. This highlights the temporal flexibility of our approach. We evaluate our proposed method $MM - VSF$ with $SM - MAE$, which is the common setting in existing remote sensing based foundation models (e.g. [5, 12]). Both $MM - VSF$ (ours) and $SM - MAE$ (widely adopted setting) return embedding series and the decoder layers including the attention mechanism

are finetuned, i.e. the encoder weights to obtain the embedding series are fixed from the respective pretraining task. Both finetuned models are trained with the same data from only the year of 2018 with their respective best hyperparameter setting.

3.3.3 Performance on downstream task. Table 2 compares the performance of $MM - VSF$ and $SM - MAE$ when finetuned on our crop mapping downstream task. We can see that when tested on test regions in the year of training, i.e 2018, the $MM - VSF$ finetuned model moderately beats the $SM - MAE$ finetuned model performing better in almost all classes, however, when testing in test regions on the next year, i.e 2019, we can see a huge improvement from our approach over $SM - MAE$. This shows the impact and generalizability of our approach over the standard approach. The fact that our embeddings when finetuned are good enough to generalise across years shows that important information has been captured in the embedding that goes beyond just the information contained in spectral imagery.

Note that with the minimal effort of choosing a time-frame for input series and adding a task-specific decoder, we adapted our $MM - VSF$ framework for the Crop-mapping downstream task. This provides empirical evidence of our framework’s flexibility to various remote-sensing based spatiotemporal tasks.

4 Conclusion

In this paper we proposed a novel multimodal spatiotemporal foundation model, $MM - VSF$, that uses multimodal input of satellite and weather data and a knowledge guided pretraining task of variable step forecasting. This leads to superior embeddings when compared with embeddings achieved by models using single modality input and trained with standard pretraining task of reconstruction. Our pretraining task evaluation of $MM - VSF$ forecasting capability showed that our foundation model is able to learn aspects that go beyond temporal autocorrelation. We showed that $MM - VSF$ can be finetuned for a crop mapping model that is generalisable across years. Our model is temporally flexible and can adapt to geoscience downstream tasks that include spatiotemporal remote-sensing data. Our study is the first step towards incorporating knowledge guided principles in pretraining tasks and adopting multimodal approaches to improve embeddings.

Acknowledgments

We acknowledge NSF Award 2313174 and NSF/NIFA NAIRI Award no. 2023-67021-39829 for funding and Minnesota Supercomputing Institute (MSI) for providing computing resources.

References

- [1] Josh Achiam, Steven Adler, Sandhini Agarwal, Lama Ahmad, Ilge Akkaya, Florencia Leoni Aleman, Diogo Almeida, Janko Altschmidt, Sam Altman, Shyamal Anadkat, et al. 2023. Gpt-4 technical report. *arXiv preprint arXiv:2303.08774* (2023).
- [2] Favien Bastani, Piper Wolters, Ritwik Gupta, Joe Ferdinando, and Aniruddha Kembhavi. 2023. Satlaspretrain: A large-scale dataset for remote sensing image understanding. In *Proceedings of the IEEE/CVF International Conference on Computer Vision*. 16772–16782.
- [3] Roberto Bentivoglio, Elvin Isufi, Sebastian Nicolaas Jonkman, and Riccardo Taormina. 2022. Deep learning methods for flood mapping: a review of existing applications and future research directions. *Hydrology and Earth System Sciences Discussions* 2022 (2022), 1–50.

- [4] Keungang Cha, Junghoon Seo, and Taekyung Lee. 2023. A billion-scale foundation model for remote sensing images. *arXiv preprint arXiv:2304.05215* (2023).
- [5] Yezhen Cong, Samar Khanna, Chenlin Meng, Patrick Liu, Erik Rozi, Yutong He, Marshall Burke, David Lobell, and Stefano Ermon. 2022. Satmae: Pre-training transformers for temporal and multi-spectral satellite imagery. *Advances in Neural Information Processing Systems* 35 (2022), 197–211.
- [6] Cheng Deng, Tianhang Zhang, Zhongmou He, Qiyuan Chen, Yuanyuan Shi, Yi Xu, Luoyi Fu, Weinan Zhang, Xinbing Wang, Chenghu Zhou, et al. 2024. K2: A foundation language model for geoscience knowledge understanding and utilization. In *Proceedings of the 17th ACM International Conference on Web Search and Data Mining*, 161–170.
- [7] Zhihan Gao, Xingjian Shi, Hao Wang, Yi Zhu, Yuyang Bernie Wang, Mu Li, and Dit-Yan Yeung. 2022. Earthformer: Exploring space-time transformers for earth system forecasting. *Advances in Neural Information Processing Systems* 35 (2022), 25390–25403.
- [8] Rahul Ghosh, Praveen Ravirathinam, Xiaowei Jia, Chenxi Lin, Zhenong Jin, and Vipin Kumar. 2021. Attention-augmented spatio-temporal segmentation for land cover mapping. In *2021 IEEE International Conference on Big Data (Big Data)*. IEEE, 1399–1408.
- [9] Xin Guo, Jiangwei Lao, Bo Dang, Yingying Zhang, Lei Yu, Lixiang Ru, Liheng Zhong, Ziyuan Huang, Kang Wu, Dingxiang Hu, et al. 2024. Skysense: A multimodal remote sensing foundation model towards universal interpretation for earth observation imagery. In *Proceedings of the IEEE/CVF Conference on Computer Vision and Pattern Recognition*, 27672–27683.
- [10] Kaiming He, Xinlei Chen, Saining Xie, Yanghao Li, Piotr Dollár, and Ross Girshick. 2022. Masked autoencoders are scalable vision learners. In *Proceedings of the IEEE/CVF conference on computer vision and pattern recognition*. 16000–16009.
- [11] Danfeng Hong, Bing Zhang, Xuyang Li, Yuxuan Li, Chenyu Li, Jing Yao, Naoto Yokoya, Hao Li, Pedram Ghamisi, Xiuping Jia, et al. 2024. SpectralGPT: Spectral remote sensing foundation model. *IEEE Transactions on Pattern Analysis and Machine Intelligence* (2024).
- [12] Johannes Jakubik, Sujit Roy, C. E. Phillips, Paolo Fraccaro, Denys Godwin, Bianca Zadrozny, Daniela Szwarzman, Carlos Gomes, Gabby Nyirjesy, Blair Edwards, Daiki Kimura, Naomi Simumba, Linsong Chu, S. Karthik Mukkavilli, Devyani Lambhate, Kamal Das, Ranjini Bangalore, Dario Oliveira, Michal Muszynski, Kumar Ankur, Muthukumar Ramasubramanian, Iksha Gurung, Sam Khallaghi, Hanxi, Li, Michael Cecil, Maryam Ahmadi, Fatemeh Kordi, Hamed Alemohammad, Manil Maskey, Raghu Ganti, Kommy Weldemariam, and Rahul Ramachandran. 2023. Foundation Models for Generalist Geospatial Artificial Intelligence. arXiv:2310.18660 [cs.CV] <https://arxiv.org/abs/2310.18660>
- [13] Samar Khanna, Patrick Liu, Linqi Zhou, Chenlin Meng, Robin Rombach, Marshall Burke, David B Lobell, and Stefano Ermon. 2023. Diffusionsat: A generative foundation model for satellite imagery. In *The Twelfth International Conference on Learning Representations*.
- [14] Nataliia Kussul, Mykola Lavreniuk, Sergii Skakun, and Andrii Shelestov. 2017. Deep learning classification of land cover and crop types using remote sensing data. *IEEE Geoscience and Remote Sensing Letters* 14, 5 (2017), 778–782.
- [15] Kentaro Kuwata and Ryosuke Shibasaki. 2015. Estimating crop yields with deep learning and remotely sensed data. In *2015 IEEE international geoscience and remote sensing symposium (IGARSS)*. IEEE, 858–861.
- [16] Fan Liu, Delong Chen, Zhangqingyun Guan, Xiaocong Zhou, Jiale Zhu, Qiaolin Ye, Liyong Fu, and Jun Zhou. 2024. Remoteclip: A vision language foundation model for remote sensing. *IEEE Transactions on Geoscience and Remote Sensing* (2024).
- [17] Gengchen Mai, Chris Cundy, Kristy Choi, Yingjie Hu, Ni Lao, and Stefano Ermon. 2022. Towards a foundation model for geospatial artificial intelligence (vision paper). In *Proceedings of the 30th International Conference on Advances in Geographic Information Systems*. 1–4.
- [18] Utkarsh Mall, Cheng Perng Phoo, Meilin Kelsey Liu, Carl Vondrick, Bharath Hariharan, and Kavita Bala. 2023. Remote sensing vision-language foundation models without annotations via ground remote alignment. *arXiv preprint arXiv:2312.06960* (2023).
- [19] Matias Mendieta, Boran Han, Xingjian Shi, Yi Zhu, and Chen Chen. 2023. Towards geospatial foundation models via continual pretraining. In *Proceedings of the IEEE/CVF International Conference on Computer Vision*. 16806–16816.
- [20] Guruprasad Nayak, Varun Mithal, Xiaowei Jia, and Vipin Kumar. 2018. Classifying multivariate time series by learning sequence-level discriminative patterns. In *Proceedings of the 2018 SIAM International Conference on Data Mining*. SIAM, 252–260.
- [21] Tung Nguyen, Johannes Brandstetter, Ashish Kapoor, Jayesh K Gupta, and Aditya Grover. 2023. ClimateX: A foundation model for weather and climate. *arXiv preprint arXiv:2301.10343* (2023).
- [22] Jaideep Pathak, Shashank Subramanian, Peter Harrington, Sanjeev Raja, Ashesh Chattopadhyay, Morteza Mardani, Thorsten Kurth, David Hall, Zongyi Li, Kamyar Azizzadenesheli, et al. 2022. Fourcastnet: A global data-driven high-resolution weather model using adaptive fourier neural operators. *arXiv preprint arXiv:2202.11214* (2022).
- [23] Praveen Ravirathinam, Rahul Ghosh, Ankush Khandelwal, Xiaowei Jia, David Mulla, and Vipin Kumar. 2024. Combining Satellite and Weather Data for Crop Type Mapping: An Inverse Modelling Approach. In *Proceedings of the 2024 SIAM International Conference on Data Mining (SDM)*. SIAM, 445–453.
- [24] Seyd Teymoor Seydi, Mahdi Hasanlou, and Jocelyn Chanusot. 2022. Burnt-Net: Wildfire burned area mapping with single post-fire Sentinel-2 data and deep learning morphological neural network. *Ecological Indicators* 140 (2022), 108999.
- [25] Amanpreet Singh, Ronghang Hu, Vedanuj Goswami, Guillaume Couairon, Wojciech Galuba, Marcus Rohrbach, and Douwe Kiela. 2022. Flava: A foundational language and vision alignment model. In *Proceedings of the IEEE/CVF Conference on Computer Vision and Pattern Recognition*. 15638–15650.
- [26] Xian Sun, Peijin Wang, Wanxuan Lu, Zicong Zhu, Xiaonan Lu, Qibin He, Junxi Li, Xuee Rong, Zhujun Yang, Hao Chang, et al. 2022. RingMo: A remote sensing foundation model with masked image modeling. *IEEE Transactions on Geoscience and Remote Sensing* 61 (2022), 1–22.
- [27] Hugo Touvron, Thibaut Lavril, Gautier Izacard, Xavier Martinet, Marie-Anne Lachaux, Timothée Lacroix, Baptiste Rozière, Naman Goyal, Eric Hambro, Faisal Azhar, et al. 2023. Llama: Open and efficient foundation language models. *arXiv preprint arXiv:2302.13971* (2023).
- [28] Gabriel Tseng, Ruben Cartuyvels, Ivan Zvonkov, Mirali Purohit, David Rolnick, and Hannah Kerner. 2023. Lightweight, pre-trained transformers for remote sensing timeseries. *arXiv preprint arXiv:2304.14065* (2023).
- [29] Di Wang, Qiming Zhang, Yufei Xu, Jing Zhang, Bo Du, Dacheng Tao, and Liangpei Zhang. 2022. Advancing plain vision transformer toward remote sensing foundation model. *IEEE Transactions on Geoscience and Remote Sensing* 61 (2022), 1–15.
- [30] Jiaxuan You, Xiaocheng Li, Melvin Low, David Lobell, and Stefano Ermon. 2017. Deep gaussian process for crop yield prediction based on remote sensing data. In *Proceedings of the AAAI conference on artificial intelligence*, Vol. 31.
- [31] Lu Yuan, Dongdong Chen, Yi-Ling Chen, Noel Codella, Xiyang Dai, Jianfeng Gao, Houdong Hu, Xuedong Huang, Boxin Li, Chunyuan Li, et al. 2021. Florence: A new foundation model for computer vision. *arXiv preprint arXiv:2111.11432* (2021).
- [32] Yi Zhao, Jiale Ma, Xiaohui Li, and Jie Zhang. 2018. Saliency detection and deep learning-based wildfire identification in UAV imagery. *Sensors* 18, 3 (2018), 712.